COMMUNICATIONS IN SCIENCE AND TECHNOLOGY
Homepage: cst.kipmi.or.id

Discovery of thymol-fused chalcones as new competitive α-glucosidase inhibitors: Design, synthesis, biological evaluation, and molecular modeling studies

Ade Danova[a,*], Elvira Hermawati[a], Warinthorn Chavasiri[b], Didin Mujahidin[a], Anita Alni[a], and Robby Roswanda[a]

[a]*Organic Chemistry Division, Department of Chemistry, Faculty of Mathematics and Natural Sciences, Institut Teknologi Bandung, Bandung 40132, Indonesia*
[b]*Center of Excellence in Natural Products Chemistry, Department of Chemistry, Faculty of Science, Chulalongkorn University, Bangkok 10330, Thailand*

Article history:
Received: 8 August 2024 / Received in revised form: 15 October 2024 / Accepted: 7 December 2024

Abstract

This study aims to synthesize and evaluate the inhibitory activity of thymol derivatives targeting α-glucosidase using *in vitro* and *in silico* studies. Ten thymol derivatives (2-11) including five new thymol-fused chalcones (7-11) were successfully synthesized. Among them, four compounds (4, 8, 9, 11) showed the best inhibitory activity with IC_{50} values of 18.45, 13.75, 8.86, and 10.67μM compared with acarbose (IC_{50} = 832.82 μM), respectively. The kinetic study of three new thymol-fused chalcones (8, 9, 11) exhibited a competitive inhibition. Molecular docking demonstrated the predicted interactions between ligand (8, 9, 11) and α-glucosidase, which are responsible for inhibiting the enzyme's catalytic abilities. Furthermore, molecular dynamics simulation of the enzyme-ligand 9 complex indicated that this complex was stable in aqueous condition. This research contributes significantly to the understanding of thymol-fused chalcones that may have therapeutic potential and their possible application in the treatment of type 2 diabetes mellitus (T2DM) for further study.

Keywords: Thymol; chalcone; diabetes mellitus; α-glucosidase; molecular docking; molecular dynamics

1. Introduction

Diabetes mellitus refers to a condition that can be caused by either insufficient use of insulin produced naturally in the body or a lack of insulin secretion due to the destruction of beta cells [1]. International Diabetes Federation (IDF) revealed that in 2019, there were 463 million cases of diabetes mellitus. This number is predicted to increase to 578 million by 2030 and 700 million by 2045 [2]. This suggests the prevalence of this disease, which is particularly high in low- and middle-income countries [3,4]. A diet rich in carbohydrates is contributing to the rise of diabetes in Asian countries, leading them to be a significant contributor to the global diabetes pandemic [5]. Elevated blood glucose levels in diabetes mellitus can lead to serious health complications, such as kidney, heart, and nervous system disorders, leg amputation, and retinopathy. These conditions not only can have a significant impact on a person's quality of life but also can result in the high levels of morbidity and mortality [6-8]. Diabetes mellitus is categorized into three types: Type I, Type II, and gestational diabetes. Type I diabetes is typically managed with insulin, while Type II and gestational diabetes are commonly managed with oral glucose-lowering drugs that work to lower blood sugar levels [9]. These drugs work through various mechanisms and are classified accordingly [10]. The main strategies involve decreasing sugar absorption by preventing the hydrolysis of carbohydrates in the gastrointestinal tract using acarbose, miglitol, and voglibose [11,12], altering the body's and cellular energy metabolism with metformin [13], elevating glucosuria via sodium-glucose co-transporter 2 (SGLT2) inhibition in the kidney with dapagliflozin, empagliflozin, and canagliflozin [14-16], reducing insulin resistance through PPARγ stimulation with rosiglitazone and pioglitazone [17,18], and stimulating insulin released from pancreatic β-cells using sulfonylureas, tolbutamide, chlorpropamide, glibenclamide, glimepiride, glipizide, gliclazide, and gliquidone [19,20].

In individuals with type 2 diabetes mellitus (T2DM), the first phase of insulin response to nutrient intake is severely impaired or absent, leading to postprandial glucose excursions most of the time [21]. Postprandial hyperglycemia is a significant risk factor for both micro- and macrovascular complications associated with diabetes mellitus [22].

* Corresponding author.
Email: adedanova@itb.ac.id
https://doi.org/10.21924/cst.9.2.2024.1497

Moreover, acute blood glucose fluctuations during the postprandial period cause more oxidative stress than chronic sustained hyperglycemia, resulting in more detrimental outcomes [23]. Managing both hemoglobin A1c and mean glucose concentration during acute glucose fluctuations, therefore, is deemed crucial for effective diabetes management. This can be achieved by delaying intestinal glucose absorption by interfering with the digestion of polysaccharides by carbohydrate digestive enzymes, particularly α-glucosidase [24]. α-Glucosidase, located at the brush border of the intestine, catalyzes the digestion of polysaccharides into absorbable glucose and is a promising target for managing postprandial hyperglycemia with insignificant side effects [25]. Currently, three α-glucosidase inhibitors, those are acarbose, voglibose, and miglitol, are available in clinical practice; they are carbohydrate mimics or iminosugar derivatives [26]. However, these carbohydrate mimics suffer from various side effects, such as bloating, nausea, diarrhea, skin allergies, and liver dysfunction, later on limiting their use in clinical practice [27, 28]. For this, the development of novel α-glucosidase inhibitors with reduced side effects and improved efficacy remains a significant focus for medicinal chemists worldwide.

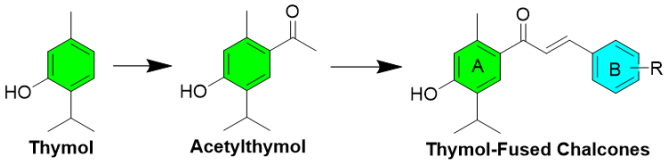

Fig. 1. Thymol and its derivatives

Natural products have so long been considered as a valuable resource for medicinal chemists, offering a diverse array of potential lead compounds for the development of drugs to treat a variety of diseases and conditions [29]. Thymol is a monoterpene (essential oil) found in *Thymus vulgaris* (30-40%) and *Origanum vulgarus* (1-30%) [30]. Thymol has been reported to show antibacterial, antifungal, larvicidal, acaricidal, and PDK3 (pyruvate dehydrogenase kinase 3) inhibitors [31-35]. Although thymol has various bioactivities, monoterpene is unstable in the formulation step in view of its volatile and strong smell [36]. Currently, many reported derivatives of thymol have shown biological properties such as thymol ester [36], thymol carbamate [37], thymol-hydrazone hybrids [38], and thymol-heterocyclic hybrids [39]. Singh et al. (2019) reported that thymol-fused chalcones and pyrazolines with thymol on the B ring exhibited a potency as antimalarial [40]. Salazar et al. (2020) reported that benzensulfonylthymol ester exhibited potent inhibitory activity against α-glucosidase with mixed-type inhibition [41]. Moreover, Singh et al. (2024) revealed that triazole-tethered thymol/carvacrol-coumarin hybrids showed promising antidiabetic without toxicity with mixed-type inhibition [42]. This study, in turn, aims to synthesize several derivatives of acetylthymol (Fig. 1) including thymol-fused chalcones with thymol on the A ring and evaluate their inhibitory activity and inhibition mechanism against α-glucosidase. Molecular docking and molecular dynamics were performed to study their binding interaction and stability of inhibitor-enzyme complexes in aqueous conditions.

2. Materials and Methods

2.1. General

Chemicals were purchased from TCI (Japan), Sigma Aldrich (Germany), and Merck (Germany). Silica gel for column chromatography (CC) with a particle size range of 0.063–0.200 mm was sourced from Merck Company. α-Glucosidase from Saccharomyces cerevisiae (EC.3.2.1.2.0), *p*-NPG (*p*-nitrophenyl-α-D-glucopyranoside), and acarbose (positive control) were obtained from Sigma Aldrich and TCI. α-Glucosidase inhibition assays were conducted using the ALLSHENG AMR-100 microplate reader. Thin-layer chromatography (TLC) was performed on Merck TLC plates with a thickness of 0.23 mm. Compounds were visualized using UV light by applying vanillin sulfate in ethanol, and by heating on a hot plate. The structure elucidation of the compounds was determined using NMR spectroscopy with a JEOL JNM-EC500R instrument operating at 500MHz. The Waters LCT Premier XE mass spectrometer was provided to obtain the data of high-resolution electrospray ionization mass spectrometry (ESI-TOF).

2.2. General procedures

2.2.1. Synthesis of 4-acetylthymol (3)

Compound 3 was synthesized using a previous method [39]. Thymol (6.0 g, 40 mmol) and pyridine (3 mL) in dichloromethane (50 mL) were mixed at 0°C. Acetyl chloride (15 mL, 210 mmol) was added to the mixture at 0°C and stirred at room temperature for 6 hours. Cold water, after the reaction completion, was added to the reaction mixture, and then 50% HCl till pH = 1-2 and no pyridine in the organic phase. The organic phase was collected and saturated $NaHCO_3$ was added until pH = 7. Subsequently, the organic phase was separated and evaporated by means of a rotary evaporator to obtain thymol acetate (2) as yellow oil without further purification.

In 20 mL nitrobenzene, thymol acetate (2) (7.7 g, 40 mmol) and acetyl chloride (2.8 mL, 40 mmol) were mixed at 0°C. Anhydrous $AlCl_3$ (8 g, 60 mmol) in 30 mL nitrobenzene was added to the reaction mixture at 0°C and stirred at room temperature for 4 hours. Cold water and 10% HCl were then added to the reaction mixture and extracted using dichloromethane. The organic phase was collected and stirred with 10% NaOH for 15 minutes. The organic layer was separated, and the polar phase was added with 10% HCl till pH = 2. The precipitate was formed, filtered, and washed with water to obtain pure 4-acetyltyhmol with yield 68.8%. The pure product was dried and characterized using NMR spectroscopy.

Compound 2. ^{1}H NMR (500 MHz, DMSO-d_6) δ_H (ppm) 7.23 (d, J = 8.0 Hz, 1H), 7.03 (dd, J = 8.0, 2.5 Hz, 1H), 6.83 (d, J = 2.0 Hz, 1H), 2.91 (Sept, J = 7.0 Hz, 1H), 2.28 (s, 3H), 2.26 (s, 3H), 1.11 (d, J = 7.0 Hz, 6H). ^{13}C NMR (125 MHz, DMSO-d_6) δ_C (ppm) 169.4, 147.7, 136.7, 136.1, 126.9, 126.3, 122.8, 26.5, 22.9, 20.6, 20.3.

Compound 3. ^{1}H NMR (500 MHz, $CDCl_3$) δ_H (ppm) 7.66 (s, 1H), 6.68 (s, 1H), 3.25 (sept, J = 7.5 Hz, 1H), 2.60 (s, 3H), 2.50 (s, 3H), 1.27 (d, J = 7.0 Hz, 6H). ^{13}C NMR (125 MHz, $CDCl_3$) δ_C (ppm) 201.2, 156.9, 139.7, 131.9, 129.9, 129.4, 119.0, 29.2, 26.9, 22.6, 22.2.

2. 2. 2. α-Bromination of 4-acetyl thymol (4)

Compound 4 was synthesized using a previous work [43]. 4-Acetyl thymol (1.5 g, 7.8 mmol) was dissolved in 20 mL AcOH, added with 1 mL Br_2 in 10 mL AcOH and stirred at room temperature for 24 hours. Afterward, 3 mL Br_2 in AcOH 10 mL was added to the reaction mixture and stirred for 24 hours. Following the reaction completion, $N_2S_2O_3$ was added to the reaction mixture and $NaHCO_3$ until pH=6. The reaction mixture was extracted using ethyl acetate and purified using column chromatography with eluent system hexane:EtOAc = 9:1. The pure product was obtained with the yield of 48.5%.

Compound 4. ^{1}H NMR (500 MHz, $CDCl_3$) δ_H (ppm) 7.51 (s, 1H), 6.60 (s, 1H), 6.24 (brs, 1H), 3.32 (sept, J = 7.0 Hz, 1H), 2.54 (s, 3H), 1.27 (d, J = 4.5 Hz, 6H). ^{13}C NMR (125 MHz, $CDCl_3$) δ_C (ppm) 187.7, 153.2, 138.5, 133.0, 126.2, 117.0, 42.4, 28.2, 22.3, 21.2. HR-ESI-TOF-MS $[M+H]^+$ m/z calc. for $C_{12}H_{14}Br_3O_2^+$: 426.8538, Found: 426.8524.

2. 2. 3. Synthesis of 6-bromo-4-acetyl thymol (5)

Compound 5 was synthesized using a previous method [44]. 4-Acetyl thymol (0.192 g, 1.0 mmol) was dissolved in 10 mL of dichloromethane and added with NBS (0.178 g, 1.0 mmol) at room temperature for 1 hour. Cold water was then added and the organic phase was separated and evaporated. The pure compound was obtained using column chromatography with hexane: EtOAc = 9:1. Here, the pure product was obtained with the yield of 80.1%.

Compound 5. ^{1}H NMR (500 MHz, DMSO-d_6) δ_H (ppm) 9.43 (s, 1H), 7.54 (s, 1H), 3.28 (sept, J = 7.0 Hz, 1H), 2.52 (s, 3H), 2.43 (s, 3H), 1.52 (d, J = 6.5 Hz, 6H). ^{13}C NMR (125 MHz, DMSO-d_6) δ_C (ppm) 200.6, 153.2, 135.3, 133.6, 131.9, 126.3, 116.8, 29.9, 27.0, 22.4, 20.6. HR-ESI-TOF-MS $[M+H]^+$ m/z calc. for $C_{12}H_{16}BrO_2^+$: 271.0328, Found: 271.0330

2. 2. 4. Synthesis of 1-O-ethoxymethoxy-4-acetyl thymol ether (6)

4-Acetylthymol (0.75 g, 3.9 mmol) was mixed with K_2CO_3 (0.81 g, 5.85 mmol) in acetone 20 mL followed by adding chloromethyl ethyl ether (0.41 g, 4.29 mmol) at room temperature. The mixture was refluxed for 24 hours. The reaction mixture was then filtered, evaporated, and purified by means of column chromatography with eluent system hexane: EtOAc = 9:1. The pure compound was obtained with the yield of 81% (0.788 g).

Compound 6. ^{1}H NMR (500 MHz, $CDCl_3$) δ_H (ppm) 7.61 (s, 1H), 6.92 (s, 1H), 5.30 (s, 2H), 3.73 (q, J = 7.5 Hz, 2H), 3.29 (sept, J = 7.0 Hz, 1H), 2.56 (s, 3H), 2.53 (s, 3H), 1.25 (s, 3H), 1.24 (t, J = 7.0 Hz, 3H), 1.24 (d, J = 7.0 Hz, 6H). ^{13}C NMR (125 MHz, $CDCl_3$) δ_C (ppm) 200.3, 157.0, 139.1, 134.4, 130.8, 128.7, 116.8, 92.8, 64.7, 29.4, 26.9, 22.7, 22.3, 15.2. HR-ESI-TOF-MS $[M+H]^+$ m/z calc. for $C_{15}H_{23}O_3^+$: 251.1642, Found: 251.1639.

2. 2. 5. Synthesis of thymol fused chalcones (7-11)

Compounds 7-11 were synthesized using a previous work [45]. 4-Acetylthymol (0.192 g, 1 mmol) in 10 mL of methanol was mixed with 1 mL of NaOH 5 M at room temperature. Substituted benzaldehydes (0.25 g, 1.5 mmol) were added to the reaction mixtures and stirred at room temperature for 1-2 days. Cold water subsequently was added to the mixtures followed by the addition of 10% of HCl until pH 2-3. The organic compound was extracted using ethylacetate and then evaporated. The compound in its purest form was isolated through column chromatography with hexane and EtOAc (9:1) as the mobile phase. The pure product was obtained with the yield of 21% (7), 47% (8), 45% (9), 38% (10), and 13% (11).

Compound 7. ^{1}H NMR (500 MHz, DMSO-d_6) δ_H (ppm) 9.92 (brs, 1H), 7.45 (s, 1H), 7.42 (d, J = 15.5 Hz, 1H), 7.38 (d, J = 2.0 Hz, 1H), 7.36 (d, J = 15.5 Hz, 1H), 7.29 (dd, J = 8.0, 2.0 Hz, 1H), 6.99 (d, J = 8.0 Hz, 1H), 6.69 (s, 1H), 3.82 (s, 3H), 3.80 (s, 3H), 3.18 (m, 1H), 2.33 (s, 3H), 1.19 (d, J = 6.5 Hz, 6H). ^{13}C NMR (125 MHz, DMSO-d_6) δ_C (ppm) 193.0, 156.9, 150.9, 149.0, 143.6, 136.7, 131.3, 129.9, 127.8, 127.6, 124.2, 122.9, 117.8, 111.7, 110.9, 55.6, 26.42, 22.3, 20.5. HR-ESI-TOF-MS $[M+H]^+$ m/z calc. for $C_{21}H_{25}O_4^+$: 341.1747, Found: 341.1744.

Compound 8. ^{1}H NMR (500 MHz, $CDCl_3$) δ_H (ppm) 7.47 (d, J = 15.5 Hz, 1H), 7.46 (s, 1H), 7.17 (d, J = 16.0 Hz, 1H), 6.71 (d, J = 2.0 Hz, 2H), 6.66 (s, 1H), 6.51 (t, J = 2.5 Hz, 1H), 3.82 (s, 6H), 3.24 (m, 1H), 2.40 (s, 3H), 1.25 (d, J = 7.0 Hz, 6H). ^{13}C NMR (125 MHz, $CDCl_3$) δ_C (ppm) 195.4, 161.1, 155.9, 144.9, 137.9, 136.9, 131.8, 131.2, 128.8, 127.1, 118.5, 106.4, 102.7, 55.5, 26.9, 22.6, 20.6. HR-ESI-TOF-MS $[M+H]^+$ m/z calc. for $C_{21}H_{25}O_4^+$: 341.1747, Found: 341.1744.

Compound 9. ^{1}H NMR (500 MHz, $CDCl_3$) δ_H (ppm) 7.43 (d, J = 16.0 Hz, 1H), 7.42 (s, 1H), 7.08 (d, J = 16.0 Hz, 1H), 6.79 (s, 2H), 6.67 (s, 1H), 3.89 (s, 3H), 3.88 (s, 3H), 3.24 (m, 1H), 2.39 (s, 3H), 1.25 (d, J = 6.5 Hz, 6H). ^{13}C NMR (125 MHz, $CDCl_3$) δ_C (ppm) 195.6, 155.8, 153.5, 145.2, 140.3, 137.5, 131.8, 131.3, 130.6, 128.1, 126.3, 118.4, 105.6, 61.1, 56.3, 26.9, 22.6, 20.5. HR-ESI-TOF-MS $[M+H]^+$ m/z calc. for $C_{22}H_{27}O_4^+$: 371.1853, Found: 371.1856.

Compound 10. $_1$H NMR (500 MHz, $CDCl_3$) δ_H (ppm) 7.85 (d, J = 16.0 Hz, 1H), 7.49 (s, 1H), 7.25 (d, J = 16.0 Hz, 1H), 7.11 (d, J = 3.0 Hz, 1H), 6.93 (dd, J = 9.0, 3.0 Hz, 1H), 6.86 (d, J = 9.0 Hz, 1H), 6.66 (s, 1H), 3.81 (s, 3H), 3.80 (s, 3H), 3.25 (sept, J = 7.0 Hz, 1H) 2.40 (s, 3H), 1.25 (d, J = 7.0 Hz, 6H). ^{13}C NMR (125 MHz, $CDCl_3$) δ_C (ppm) 196.1, 155.7, 153.6, 153.2, 140.5, 137.9, 131.7, 131.3, 128.6, 127.6, 124.6, 118.5, 117.3, 113.5, 112.5, 55.9, 26.8, 22.6, 20.6.

Compound 11. ^{1}H NMR (500 MHz, DMSO-d_6) δ_H (ppm) 9.95

brs, 1H), 7.63 (s, 1H), 7.62 (d, *J* = 15.5 Hz, 1H), 7.48 (s, 1H), 7.34 (d, *J* = 16.5 Hz, 1H), 6.89 (d, *J* = 9.0 Hz, 1H), 6.70 (s, 1H), 3.85 (s, 3H), 3.82 (s, 3H), 3.76 (s, 3H), 3.19 (sept, *J* = 7.0 Hz,1H), 2.33 (s, 3H), 1.19 (d, *J* = 7.0 Hz, 6H). ^{13}C NMR (125 MHz, DMSO-*d*$_6$) δ_C (ppm) 192.8, 157.0, 155.5, 152.8, 141.8, 137.6, 136.9, 131.3, 129.7, 127.8, 124.9, 123.4, 121.0, 117.9, 108.5, 61.4, 60.5, 56.0, 26.3, 22.3, 20.6. HR-ESI-TOF-MS $[M+H]^+$ m/z calc. for $C_{22}H_{27}O_4^+$: 371.1853, Found: 371.1855.

2.3. Biological assay

The assay for α-glucosidase activity was performed using a method previously described [45]. In this assay, α-glucosidase (0.1 U/mL) and *p*-nitrophenyl-α-D-glucopyranoside substrate (1 mM) were dissolved in 0.1 M of phosphate buffer (pH 6.9). A 10µL sample was incubated with 40µL of α-glucosidase at 37°C for 10 min. Afterward, 50µL of the substrate solution was added to the reaction mixture, which was then incubated at 37°C for an additional 20 min before stopping by adding 100µL of Na_2CO_3 (1 M). The α-glucosidase activity was measured at 405 nm using an ALLSHENG AMR-100 microplate reader. The percentage inhibition of activity was calculated using the following formula: % inhibition = $[(A_0 - A_1)/A_0] \times 100$, where A_0 represents the absorbance in the absence of the sample and A_1 refers to the absorbance in the presence of the sample. The IC_{50} value was determined by plotting the % inhibition versus concentration. Here, acarbose was used as standard control, and the experiments were performed in triplicate. To determine α-glucosidase inhibition, a kinetic study was conducted by assessing the type of α-glucosidase inhibition at various concentrations of *p*-NPG substrate in the absence or presence of different concentrations of the test compounds. Km and Vmax values were calculated based on the Lineweaver-Burk plots of 1/V versus 1/[S].

2.3. Molecular modeling

The drawing and refinement of the compound's molecular structures were carried out using the molecular mechanics energy minimization method with the Merck molecular force field (MMFF94) in ChemOffice Professional 15.0. Due to the absence of the crystallographic structure of Saccharomyces cerevisiae lysosomal α-glucosidase (UniProt ID: P53341) in the protein data bank, the protein's structure and binding site were predicted and created using AlphaFold from https://prankweb.cz/ [46,47]. The AutoDock Vina tool in PyRx V.1.1 software was used to perform molecular docking [48, 49] with an exhaustiveness of 32 and a mode value of 9 poses for each docked ligand. The binding site of α-glucosidase was defined as a box with the dimensions of 20 Å × 20 Å × 20 Å, located at x= 11.1297, y= 3.5054, and z= -0.7673. The final step was performed by conducting binding interaction analysis and visualizing the docking results in 3D using BIOVIA Discovery Studio Visualizer.

Meanwhile, the molecular dynamics (MD) simulations were performed using YASARA software version 21.16.17 and the AMBER14 forcefield [50-52]. In these simulations, the md_run.mcr macros were utilized. The integration time, or timestep used was 2 x 1.25 fs, and the simulation duration was set to 100 ns. The MD simulations were designed to include a temperature of 298 K, a pressure of 1 bar, Coulomb electrostatics with a 7.86 cutoff, a solvent density of 0.997, a pH of 7.0, and periodic boundaries within a single simulation box containing 0.9% NaCl. Throughout the simulations, data and trajectories were recorded at the regular intervals of 100ps, allowing for the monitoring and analysis of the system behavior.

3. Results and Discussion

3.1. Synthesis

Ten thymol derivatives were synthesized including thymol ethanoate (2), 4-acetyltyhmol (3), and its derivatives (4-6) as well as five new thymol-fused chalcones (7-11). As shown in Fig. 2, all thymol derivatives were synthesized. Moreover, the synthesized thymol derivatives were characterized using various analytical techniques, such as ^{1}H and ^{13}C Nuclear Magnetic Resonance (NMR), and for new compounds using high-resolution mass spectrometry (HR-MS) as an additional technique. The use of these techniques aimed to evaluate the properties of the synthesized compounds. The experimental section outlines the procedure used to synthesize thymol derivatives and provides spectral information for these compounds, which align with their designated structures.

In this study, as presented in Fig. 3 and 4, thymol-fused chalcone of compound 9 was chosen for addressing the structural elucidation. The ^{1}H NMR presented two new signals of doublets at 7.08 and 7.43 ppm related to two protons of sp^2 with the trans configuration of chalcone with coupling constant at 16.0 Hz. The ^{13}C NMR showed one signal at 195.6 ppm related to conjugated carbonyl, twelve signals at 105.6-155.8 ppm related to carbon of sp^2, and five signals at 20.5-61.1 ppm related to carbon of sp^3. Furthermore, high resolution mass spectrometry (HRMS) was conducted to obtain m/z 371.1856 $[M+H]^+$ (calc. for $C_{22}H_{27}O_4^+$: 371.1853).

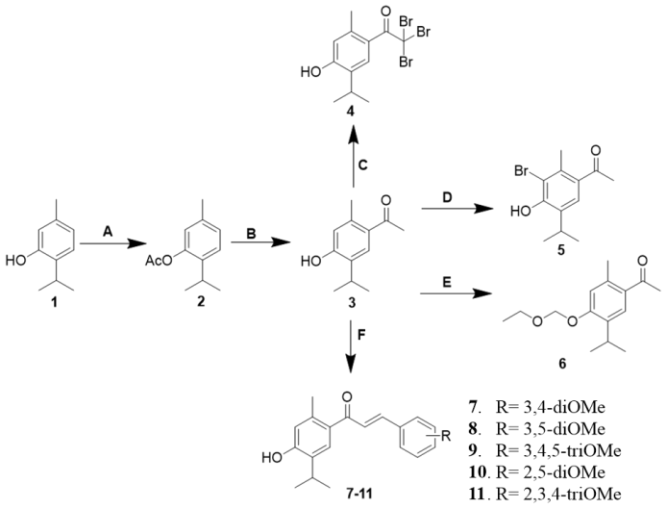

Fig. 2. Reagent and conditions: A) AcCl, DMF, pyridine, rt; B) nitrobenzene, AcCl, $AlCl_3$, 10°C-rt; C) Br_2 excess, AcOH, rt; D) NBS, DCM, rt, 2 hrs.; E) acetone, K_2CO_3, reflux, 24 hrs.; F) NaOH 5 M, MeOH, rt, 48 hrs

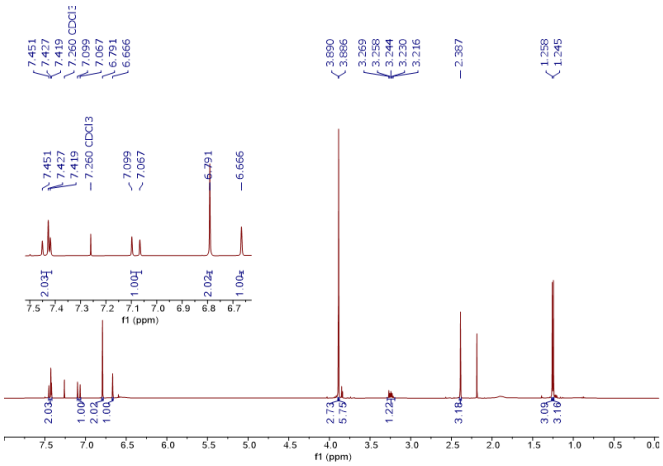

Fig. 3. ^{1}H NMR spectrum (500 MHz) of 9 in $CDCl_3$

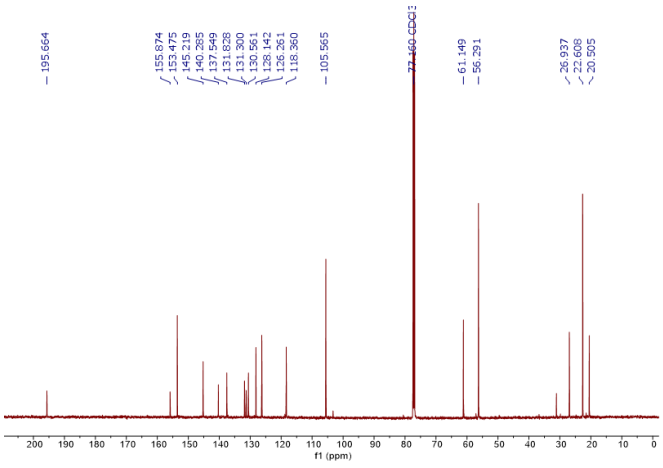

Fig. 4. ^{13}C NMR spectrum (125 MHz) of 9 in $CDCl_3$

3.2. Biological evaluation

Thymol (1) and its derivatives (2-11) were evaluated for inhibitory activity against α-glucosidase enzyme. First, all compounds were screened at 50 µM against α-glucosidase enzyme. Among thymol (1) and five derivatives (2-6), five compounds (1, 2, 5, 6) did not inhibit the enzyme, except compounds 3 and 4 from low to strong inhibition as presented in Table 1. This study showed that the modification of 4-acetyl thymol (3) on α-carbon exhibited good inhibitory activity against α-glucosidase enzyme. This study, therefore, synthesized thymol-fused chalcones considering that chalcones are simple structures possessing unsaturated ketone as a linker between two aromatic rings providing wide biological spectrum [45]. Moreover, thymol-fused chalcones were performed for further evaluation. Compounds (7-11) were screened at 50 µM with the result showing that three compounds (8, 9, and 11) exhibited a strong inhibitory activity more than 70%, and two compounds (7, and 10) showed low inhibition less than 60% as shown in Table 1. Compounds with inhibition more than 70% were further evaluated to obtain IC_{50}. The result of four selected compounds (4, 8, 9, and 11) showed strong inhibition against α-glucosidase with IC_{50} values approximately 18.45, 13.75, 8.86, and 10.67 µM, respectively, compared to acarbose as presented in Table 1. This study suggested that the presence of unsaturated ketone and the methoxy group could be crucial to maintain the inhibitory activity against α-glucosidase in the active site [45].

Table 1. *In vitro* α-glucosidase inhibitory activity of compounds 1-11 and acarbose

Compound	%Inhibition (50 µM)[a]	IC_{50} (µM)[a]
1	[b]NI	-
2	[b]NI	-
3	31.69±2.72	-
4	77.21±3.52	18.45±2.52
5	1.58±0.17	-
6	[b]NI	-
7	57.32±9.31	-
8	71.14±1.73	13.75±1.41
9	73.66±8.86	08.86±1.12
10	43.72±4.49	-
11	83.97±5.27	10.67±2.21
Acarbose	-	832.82±46.35

[a]The data were calculated from triplicate as mean±SD. [b]NI = no inhibition.

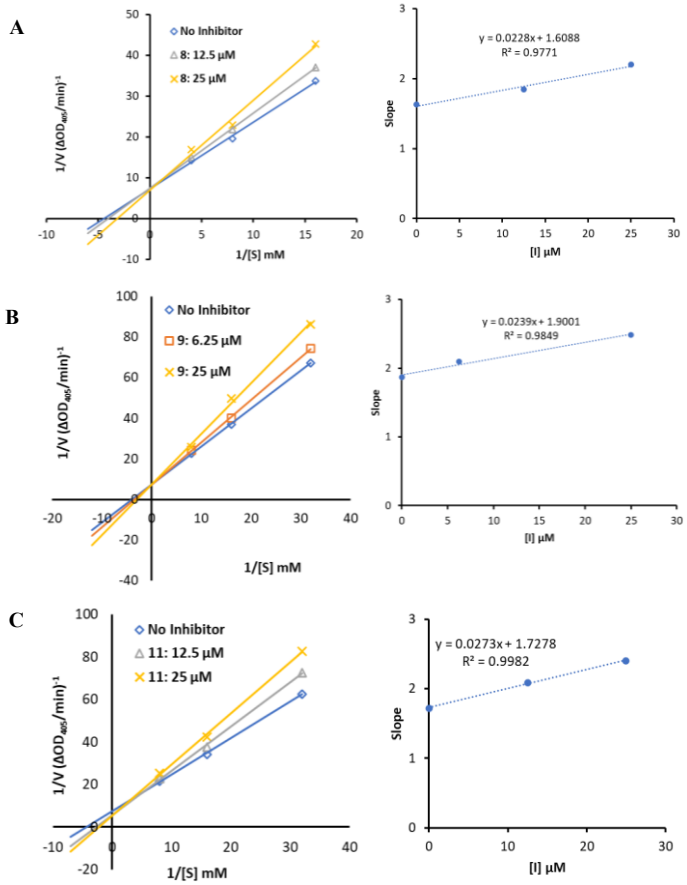

Fig. 5. The Lineweaver–Burk plots and inhibition constant determination for compounds 8 (A), 9 (B), and 11 (C)

The kinetic study was performed on the best inhibitory activity of thymol-fused chalcones to further evaluate the mechanism of inhibition. Three compounds (8, 9, and 11) were selected for kinetic study. Fig. 5 presents the summary

of the kinetic study in which the result showed that three selected compounds (8, 9, and 11) exhibited a competitive inhibition by increasing both K_m and V_{max} values dependent upon the concentration of the compound against α-glucosidase. Moreover, the inhibition constant (K_i) values of three compounds exhibited at 70.56, 79.50, and 63.29 μM, respectively. Meanwhile, other reports showed that chalcones and their hybrids showed competitive and mixed-type inhibition against α-glucosidase [45, 53-56].

3.3. Molecular modeling

3.3.1. Molecular docking

Molecular docking studies were conducted purposely to predict the binding interactions of the synthesized compounds at the active site of the α-glucosidase enzyme from Saccharomyces cerevisiae. Previous research involving similar compounds indicated that the binding sites of acarbose and the selected compounds were similar [57, 58]. This study focused on the docking process at the catalytic site of α-glucosidase, which included catalytic triads consisting of Asp214, Glu276, and Asp349. Additionally, several amino acid residues, such as Lys155, Phe157, Phe158, Phe177, Thr215, Leu218, Ala278, and Arg312, were identified as flanking the catalytic triads, thereby facilitating non-covalent interactions between the enzyme, substrate, and inhibitor at the active site [57].

The binding mode of the screened compounds (4, 7-11) with acarbose in complex with α-glucosidase was investigated. As illustrated in Table 2, the interaction energy of compounds 7 (-8.6 kcal/mol), 8 (-9.1 kcal/mol), 9 (-9.7 kcal/mol), 10 (-9.5 kcal/mol), and 11 (-9.1 kcal/mol) was found lower than that of acarbose (-8.3 kcal/mol), except for compound 4 (-7.3 kcal/mol).

Table 2 presents the analysis of the two-dimensional (2D) interaction profile of each ligand in the active site of α-glucosidase. The results indicated that five compounds (4, 8-11) could interact with the catalytic site of α-glucosidase, except for compound 7. Compound 4 formed hydrogen bonds and π-anion interactions between the hydroxy and aromatic rings of Asp214 and Asp349. Compound 7 with two methoxy groups at the 3 and 4 positions on the B ring did not interact with the catalytic site, but still formed a hydrogen bond with Arg312, a π-π interaction with Phe300, and π-alkyl interactions with Ala278 and Arg312 located in the active site of α-glucosidase. Consequently, the inhibitory activity of compound 7 was lower than that of compound 4, as demonstrated by the in vitro test as presented in Table 1. Additionally, compound 8, with two methoxy groups at the 3 and 5 positions on the B ring, showed two interactions in the catalytic site, including π-anion and van der Waals (vdW) forces between the B ring and the methoxy group with Asp349 and Asp214, respectively. When compared to compound 8, compound 9 that had three methoxy groups at positions 3, 4, and 5 on the B ring exhibited hydrogen bond and π-anion interactions between the hydroxy and A ring with Asp214 and Asp349, respectively. Furthermore, compound 10 exhibited similar properties to compound 9 in forming hydrogen bonds and π-anion interactions with Asp214 and Asp349 in the catalytic site. However, the inhibitory activity of compound 10 was found lower than that of compound 9 in view of steric clash interaction with Glu276. Meanwhile, compound 11 exhibited hydrogen bond and π-anion interactions with the hydroxy group and the A ring, respectively with Asp214 and Asp349 in the catalytic site. As shown in Table 1, vdW interactions were found to stabilize the binding between ligands and α-glucosidase in the catalytic site for compounds 8, 9, 11, and acarbose. The results, as presented in Table 2, revealed that compounds 8, 9, and 11 exhibited greater α-glucosidase inhibitory activity than the one in compounds 3 and 4. The structural findings provide evidence for this increased activity.

The results of our study suggest that compounds 8, 9, and 11 can bind both the catalytic site (comprised of Asp214 and Asp349) and amino residues located within the active site of α-glucosidase. This indicates that these compounds are competitive inhibitors, as demonstrated by our *in vitro* test, as shown in Fig. 5.

Table 2. The docking result of the six synthesized compounds and acarbose in the α-glucosidase active site

Compound	Binding Affinity (kcal/mol)	Binding Interactions of Residues
4	-7.3	H-bond = Asp214, Arg314 π-anion = Asp349; π-σ = Tyr7; π-alkyl = Phe177
7	-8.6	H-bond = Arg312 π-π = Phe300; π-alkyl = Ala278, Arg312 H-bond = Asn241, Arg439
8	-9.1	π-anion = Asp349; π-π = Phe157; π-alkyl = Ala278, His111, Phe177, Tyr71; vdW = Asp408, Ser156, Phe157
9	-9.7	H-bond = Arg312, Asp214 π-anion = Asp349; π-σ = Phe177, Tyr71; π-alkyl = His239, Phe311, Arg312; vdW = Phe157, Pro309, His279, Glu304
10	-9.5	H-bond = Asp214; Sterich clash = Glu279 π-anion = Asp349; π-σ = Phe177, Tyr71; π-alkyl = Arg312, Tyr313, Phe311, Phe157, His279, His239
11	-9.1	H-bond = Asp214 π-anion = Asp349; π-σ = Phe177, Tyr71; π-π = Phe157; π-alkyl = Arg312; vdW = Glu304, Phe158
Acarbose	-8.3	H-bond = His279, Glu276, Glu 304, Phe157 π-σ = His239; vdW = Pro309, Arg312, Glu304

3.3.2. Molecular dynamics

The Root Mean Square Deviation (RMSD) values evaluate the divergence of the enzyme-ligand complex's structure from its initial form, reflecting the extent of flexibility and fluctuation within the complex. As depicted in Fig. 6, the

typical RMSD for ligand 9 exhibited variability until achieving stability at approximately 1.95 Å. The RMSD value for ligand 9 was found less than that of triazole-tethered carvacrol-coumarin hybrids at roughly 4.8 Å [42]. This outcome indicated that ligand 9 demonstrated greater stability. Moreover, the RMSD for the enzyme-ligand 9 complex and the enzyme-acarbose complex were observed to progressively rise until they stabilized at approximately 2.14 Å and 1.83 Å, respectively. These findings were further supported by the highest number of contacts and the Rg values (a measure of compactness) of the enzyme-ligand 9 complex throughout the simulation period, as depicted in Fig. 6. These outcomes collectively illustrate that the molecular complexation between compound 9 and α-glucosidase is remarkably stable when submerged in an aqueous environment.

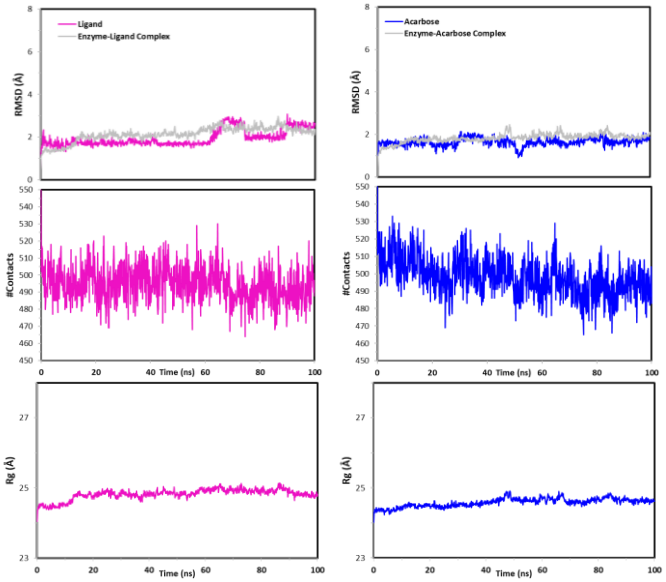

Fig. 6. Evolution of RMSD, #contacts, and Rg of ligand 9 and acarbose in complex with the α-glucosidase

4. Conclusion

In summary, ten thymol derivatives including thymol ethanoate (2), 4-acetyltyhmol (3), and its derivatives (4-6) as well as five new thymol-fused chalcones (7-11) were successfully synthesized. Among them, four compounds (4, 8, 9, and 11) exhibited strong inhibitory activity against α-glucosidase with IC_{50} values at 18.45, 13.75, 8.86, and 10.67 µM, respectively, compared to acarbose (IC_{50} = 832.82 µM). The kinetic study of three thymol-fused chalcones (8, 9, and 11) exhibited competitive inhibition against α-glucosidase. Furthermore, the result of molecular docking demonstrated a binding interaction of compound 8, 9, and 11 with residues in the catalytic site via hydrogen bond and π-anion interactions and stabilized by van der Walls interaction around the active site of α-glucosidase. Moreover, the molecular dynamics simulation of the enzyme-ligand 9 was highly stable in an aqueous condition based on the RMSD, #contact, and Rg values. Thus, thymol-fused chalcones have demonstrated potential as α-glucosidase inhibitors for addressing postprandial hyperglycemia and warrant additional investigation.

Acknowledgements

This research was funded by PPMI KK Kimia Organik FMIPA Institut Teknologi Bandung 2024 with contract number FMIPA.PPMI-KK-PN-03-2024, and the integrated chemistry laboratory for NMR spectroscopy and mass spectrometry determination. The author thanks to Ministry Education, Culture, Research, and Technology, the Republic of Indonesia through Inter University Center for Excellence (PUAPT) program and the Center of Excellence in Natural Products Chemistry, Chulalongkorn University, Thailand that have provided chemicals and biological assay.

References

1. Association AD. *Diagnosis and classification of diabetes mellitus*. Diabetes care. 2013;36:S67-S74.
2. Saeedi P, Petersohn I, Salpea P, Malanda B, Karuranga S, Unwin N, et al. *Global and regional diabetes prevalence estimates for 2019 and projections for 2030 and 2045*: Results from the International Diabetes Federation Diabetes Atlas, 9th edition. Diabetes Res. Clin. Pract. 2019;157:107843.
3. Gaziano TA, Bitton A, Anand S, Abrahams-Gessel S, Murphy A. *Growing Epidemic of Coronary Heart Disease in Low- and Middle-Income Countries*. Curr. Probl. Cardiol. 2010;35:72-115.
4. Lam AA, Lepe A, Wild SH, Jackson C. *Diabetes comorbidities in low- and middle-income countries: an umbrella review*. J. Glob. Health. 2021;11.
5. Hu FB. *Globalization of Diabetes: The role of diet, lifestyle, and genes*. Diabetes Care. 2011;34:1249-57.
6. Yen F-S, Wei JC-C, Shih Y-H, Hsu C-C, Hwu C-M. *The Risk of Nephropathy, Retinopathy, and Leg Amputation in Patients With Diabetes and Hypertension: A Nationwide, Population-Based Retrospective Cohort Study*. Front. Endocrinol. 2021;12. endo.2021.756189.
7. Aras RA, Lestari T, Nugroho HA, Ardiyanto I. *Segmentation of retinal blood vessels for detection of diabetic retinopathy: A review*. Commun. Sci. Technol. 2016;1(1).
8. Yulyanti V, Adi Nugroho H, Ardiyanto I, Oktoeberza, WK. *Dark lesion elimination based on area, eccentricity and extent features for supporting haemorrhages detection*. Commun. Sci. Technol. 2019;4(1):7-11.
9. American Diabetes A. *Diagnosis and Classification of Diabetes Mellitus*. Diabetes Care .2010;33:S62-S9.
10. El-Abhar HS, Schaalan MF. *Phytotherapy in diabetes: Review on potential mechanistic perspectives*. World J. Diabetes. 2014;5:176.
11. Trapero A, Llebaria A. A *Prospect for Pyrrolidine Iminosugars as Antidiabetic α-Glucosidase Inhibitors*. J. Med. Chem. 2012;55:10345-6.
12. Kim DK, Lee B-H. *New glucogenesis inhibition model based on complete α-glucosidases from rat intestinal tissues validated with various types of natural and pharmaceutical inhibitors*. J. Sci. Food Agric. 2022;102:4419-24.
13. Salani B, Rio AD, Marini C, Sambuceti G, Cordera R, Maggi D. *Metformin, cancer and glucose metabolism*. Endocr. Relat. Cancer. 2014;21(6):R461-R71.
14. Zhao Y, Xu L, Tian D, Xia P, Zheng H, Wang L, et al. *Effects of sodium-glucose co-transporter 2 (SGLT2) inhibitors on serum uric acid level: A meta-analysis of randomized controlled trials*. Diabetes Obes. Metab. 2018;20(2):458-62.
15. Fitchett D. *A safety update on sodium glucose co-transporter 2 inhibitors*.

Diabetes Obes. Metab. 2019;21:34-42.
16. Herrington WG, Savarese G, Haynes R, Marx N, Mellbin L, Lund LH, et al. *Cardiac, renal, and metabolic effects of sodium–glucose co-transporter 2 inhibitors: a position paper from the European Society of Cardiology ad-hoc task force on sodium–glucose co-transporter 2 inhibitors*. Eur. J. Heart Fail. 2021;23:1260-75.
17. Grygiel-Górniak B. *Peroxisome proliferator-activated receptors and their ligands: nutritional and clinical implications - a review*. Nutr. J. 2014;13:17.
18. Janani C, Ranjitha Kumari BD. *PPAR gamma gene – A review*. Diabetes Metabol Syndr: Clin. Res. Rev. 2015;9:46-50.
19. Derosa G, Maffioli P. *Management of diabetic patients with hypoglycemic agents
 α-Glucosidase inhibitors and their use in clinical practice*. Arch. Med. Sci. 2012;8:899-906.
20. Vanderlaan EL, Nolan JK, Sexton J, Evans-Molina C, Lee H, Voytik-Harbin SL. *Development of electrochemical Zn2+ sensors for rapid voltammetric detection of glucose-stimulated insulin release from pancreatic β-cells*. Biosens. Bioelectron. 2023;235:115409.
21. Altuntaş Y. *Postprandial reactive hypoglycemia*. Şişli Etfal Hastanesi tip Bülteni. 2019;53:215-20.
22. Chawla A, Chawla R, Jaggi S. *Microvasular and macrovascular complications in diabetes mellitus: Distinct or continuum?*. Indian J. Endocrinol. Metab. 2016;20.
23. Monnier L, Mas E, Ginet C, Michel F, Villon L, Cristol J-P, et al. *Activation of Oxidative Stress by Acute Glucose Fluctuations Compared With Sustained Chronic Hyperglycemia in Patients With Type 2 Diabetes*. JAMA. 2006;295:1681-7.
24. Wright LA-C, Hirsch IB. *Metrics Beyond Hemoglobin A1C in Diabetes Management: Time in Range, Hypoglycemia, and Other Parameters*. Diabetes Technol. Ther. 2017;19:S-16-S-26. https://doi.org/10.1089/dia.2017.0029.
25. Hossain U, Das AK, Ghosh S, Sil PC. *An overview on the role of bioactive α-glucosidase inhibitors in ameliorating diabetic complications*. Food Chem. Toxicol. 2020;145:111738.
26. Ghani U. *Re-exploring promising α-glucosidase inhibitors for potential development into oral anti-diabetic drugs: Finding needle in the haystack*. Eur. J. Med. Chem. 2015;103:133-62.
27. Padhi S, Nayak AK, Behera A. *Type II diabetes mellitus: a review on recent drug based therapeutics*. Biomed. Pharmacother. 2020;131:110708.
28. Singh A, Singh K, Sharma A, Kaur K, Kaur K, Chadha R, et al. *Recent developments in synthetic α-glucosidase inhibitors: A comprehensive review with structural and molecular insight*. J. Mol. Struct. 2023;1281:135115.
29. Dias DA, Urban S, Roessner U. *A Historical Overview of Natural Products in Drug Discovery*. Metabolites. 2012, p. 303-36.
30. Youssefi MR, Moghaddas E, Tabari MA, Moghadamnia AA, Hosseini SM, Farash BR, et al. *In Vitro and In Vivo Effectiveness of Carvacrol, Thymol and Linalool against Leishmania infantum*. Molecules. 2019.
31. Kachur K, Suntres Z. *The antibacterial properties of phenolic isomers, carvacrol and thymol*. Crit. Rev. Food Sci. Nutr. 2020;60:3042-53.
32. Wang K, Jiang S, Yang Y, Fan L, Su F, Ye M. *Synthesis and antifungal activity of carvacrol and thymol esters with heteroaromatic carboxylic acids*. Nat. Prod. Res. 2019;33:1924-30.
33. López V, Cascella M, Benelli G, Maggi F, Gómez-Rincón C. *Green drugs in the fight against Anisakis simplex—larvicidal activity and acetylcholinesterase inhibition of Origanum compactum essential oil*. Parasitol Res. 2018;117:861-7.
34. Araújo LX, Novato TPL, Zeringota V, Matos RS, Senra TOS, Maturano R, et al. *Acaricidal activity of thymol against larvae of Rhipicephalus microplus (Acari: Ixodidae) under semi-natural conditions*. Parasitol Res. 2015;114:3271-6.
35. Jairajpuri DS, Khan S, Anwar S, Hussain A, Alajmi MF, Hassan I. *Investigating the role of thymol as a promising inhibitor of pyruvate dehydrogenase kinase 3 for targeted cancer therapy*. Int. J. Biol. Macromol. 2024;259:129314.
36. Dominguez-Uscanga A, Aycart DF, Li K, Witola WH, Andrade Laborde JE. *Anti-protozoal activity of Thymol and a Thymol ester against Cryptosporidium parvum in cell culture*. Int. J. Parasitol. Drugs Drug Resist. 2021;15:126-33.
37. Kurt BZ, Gazioglu I, Dag A, Salmas RE, Kayık G, Durdagi S, et al. *Synthesis, anticholinesterase activity and molecular modeling study of novel carbamate-substituted thymol/carvacrol derivatives*. Bioorg. Med. Chem. 2017;25:1352-63.
38. Rajput JD, Bagul SD, Bendre RS. *Design, synthesis, biological screenings and docking simulations of novel carvacrol and thymol derivatives containing acetohydrazone linkage*. Res. Chem. Intermed. 2017;43:4893-906.
39. Nagle PS, Pawar YA, Sonawane AE, Bhosale SM, More DH. *Synthesis and evaluation of antioxidant and antimicrobial properties of thymol containing pyridone moieties*. Med. Chem. Res. 2012;21:1395-402.
40. Raghuvanshi DS, Verma N, Singh SV, Khare S, Pal A, Negi AS. *Synthesis of thymol-based pyrazolines: An effort to perceive novel potent-antimalarials*. Bioorg. Chem. 2019;88:102933.
41. Salazar MO, Osella MI, Arcusin DEJ, Lescano LE, Furlan RLE. *New α-glucosidase inhibitors from a chemically engineered essential oil of Origanum vulgare L*. Ind. Crop. Prod. 2020;156:112855.
42. Singh A, Singh K, Kaur K, Sharma A, Mohana P, Prajapati J, et al. *Discovery of triazole tethered thymol/carvacrol-coumarin hybrids as new class of α-glucosidase inhibitors with potent in vivo antihyperglycemic activities*. Eur. J. Med. Chem. 2024;263:115948.
43. Bachelet J, Cavier R, Lemoine J, Rigothier M, Gayral P, Royer R. *Comparison of the antibacterial, antiparasitic and molluscicidal properties of halogenoacylamide or halogenoacyl derivatives of thymol*.NA. Eur. J. Med. Chem. 1979;14:321-4.
44. Hengphasatporn K, Garon A, Wolschann P, Langer T, Yasuteru S, Huynh TNT, et al. *Multiple Virtual Screening Strategies for the Discovery of Novel Compounds Active Against Dengue Virus: A Hit Identification Study*. Sci. Pharm. 2020.
45. Danova A, Pattanapanyasat K, Hengphasatporn K, Shigeta Y, Rungrotmongkol T, Hermawati E, et al. *Unlocking E-arylidene Steroid Derivatives as Promising α-Glucosidase Inhibitors*. ChemistrySelect. 2024;9(9):e202303887.
46. Jakubec D, Skoda P, Krivak R, Novotny M, Hoksza D. *PrankWeb 3: accelerated ligand-binding site predictions for experimental and modelled protein structures*. Nucleic Acids Res. 2022;50(W1):W593-W7.
47. Yamamoto K, Miyake H, Kusunoki M, Osaki S. *Steric hindrance by 2 amino acid residues determines the substrate specificity of isomaltase from Saccharomyces cerevisiae*. J. Biosci. Bioeng. 2011;112:545-50.
48. Dallakyan S, Olson AJ. Small-Molecule Library Screening by Docking with PyRx. In: Hempel JE, Williams CH, Hong CC, editors. *Chemical Biology: Methods and Protocols*, New York, NY: Springer New York; 2015, p. 243-50.
49. Trott O, Olson AJ. *AutoDock Vina: Improving the speed and accuracy of docking with a new scoring function, efficient optimization, and multithreading*. J. Comput. Chem. 2010;31(2):455-61.
50. Duan Y, Wu C, Chowdhury S, Lee MC, Xiong G, Zhang W, et al. *A point-charge force field for molecular mechanics simulations of proteins based on condensed-phase quantum mechanical calculations*. J. Comput. Chem. 2003;24:1999-2012.

51. Krieger E, Darden T, Nabuurs SB, Finkelstein A, Vriend G. *Making optimal use of empirical energy functions: Force-field parameterization in crystal space*. Proteins. 2004;57:678-83.
52. Krieger E, Vriend G. *New ways to boost molecular dynamics simulations*. J. Comput. Chem. 2015;36:996-1007.
53. Al-ghulikah HA, Mughal EU, Elkaeed EB, Naeem N, Nazir Y, Alzahrani AY, Sadiq A, Shah SW. *Discovery of chalcone derivatives as potential α-glucosidase and cholinesterase inhibitors: Effect of hyperglycemia in paving a path to dementia*. J. Mol. Struct. 2023;1275:134658.
54. Hosseini Nasab N, Raza H, Eom YS, Shah FH, Kwak JH, Kim SJ. *Exploring chalcone-sulfonyl piperazine hybrids as anti-diabetes candidates: design, synthesis, biological evaluation, and molecular docking study*. Mol. Divers. 2024;22:1-7.
55. Hu CM, Luo YX, Wang WJ, Li JP, Li MY, Zhang YF, Xiao D, Lu L, Xiong Z, Feng N, Li C. *Synthesis and evaluation of coumarin-chalcone derivatives as α-glucosidase inhibitors*. Front. Chem. 2022;10:926543.
56. He XF, Chen JJ, Li TZ, Hu J, Zhang XM, Geng CA. *Diarylheptanoid-chalcone hybrids with PTP1B and α-glucosidase dual inhibition from Alpinia katsumadai*. Bioorg. Chem. 2021;108:104683.
57. Halim SA, Jabeen S, Khan A, Al-Harrasi A. *Rational Design of Novel Inhibitors of α-Glucosidase: An Application of Quantitative Structure Activity Relationship and Structure-Based Virtual Screening*. Pharmaceuticals. 2021.
58. Ardiansah B, Rohman N, Nasution MAF, Tanimoto H, Cahyana AH, Fadlan A, et al. *Synthesis, α-Glucosidase Inhibitory Activity and Molecular Docking Study of Chalcone Derivatives Bearing a 1H-1,2,3-Triazole Unit*. Chem. Pharm. Bull. 2023;71:342-8.